旋轉失速實驗量測與控制

Measurement and Control of Rotating Stall

計劃編號：NSC 88-2212-E-002 -054

執行期限：87 年 8 月 1 日至 88 年 7 月 31 日

主持人：胡文聰 國立台灣大學應用力學研究所

一、中文摘要

本計劃針對台大應用力學研究所之大型、低速軸流壓縮机設備進行流場旋轉失速之實驗探討。實驗目的為針對此複雜流場進行初步之瞭解，特別在穩定流初步進入旋轉失速時之特徵現象。實驗中裝置熱線在轉子葉片前約一弦長處(為避免轉子葉片勢流場之干擾)，量測在轉子/定子壓縮段中接近失速前之流場特性。結果明確顯示進入失速前之流場為非定常，並有一段前波(precursor wave)**出現。前波之物理特性證實為旋轉失速現象之前身，亦前波直接發展至失速流場。熱線量測結果顯示旋轉失速之頻率為**93%**軸轉速，可知在本壓縮機中轉子失速現象為單失速區。**

關鍵詞: **軸流壓縮機、勢流效應。**

Abstract

Experimental study was conducted on measurement of rotating stall in the large-scale, low-speed axial compressor facility. The purpose of the study was to make initial attempt to characterize the overall phenomenon of rotating stall by measurement of hot-wire signature upstream of the rotor row. Measurement was taken at stall-onset flow coefficient with rotor/stator blade configuration. Data show clear characteristic of time-mean steady flow entering into rotating stall flow. The precursor region shows a clear growth of the instability and finally developing into a full-scale rotating stall phenomenon. The frequency of the stall cell is shown to be 0.93 that of the shaft frequency, which means that one stall cell per rev characterize this axial compressor. Moreover the signature of the hot-wire suggests that the spatial extent of the stall cell is fairly small.

Keywords: rotating stall, axial compressor, hot-wire measurement.

二、緣由與目的

There are two basic modes of instability in axial compressors - surge and rotating stall. Lavrich (1988) illustrates a compressor characteristic under surge and rotating stall. As the throttle of the compression system is reduced beyond the stable flow regime, one of the two types of instabilities develops. Surge is characterized by large amplitude and low frequency oscillation in both pressure rise and mass flow rate over the entire cross-sectional flow area. Experimental data illustrating the behavior of surge on a high pressure missile fuel pump model was published by Wo and Bons (1994). The magnitude of the oscillation suggests that the system response can be highly nonlinear. Rotating stall exhibits itself when the compressor is delivering a substantially lower pressure rise than that at design. When this flow state is encountered in actual engine operation, it is often difficult to return to the unstalled condition due to complicated blade stalling dynamics (part-span or full-span stall cells).

Experimental study was conducted on measurement of rotating stall in the large-scale, low-speed axial compressor facility. The purpose of the study was to make initial attempt to characterize the overall phenomenon of rotating stall by measurement of hot-wire signature upstream of the rotor row. Measurement was taken at stall-onset flow coefficient with rotor/stator blade configuration.

三、研究方法

The experimental compressor is a low-speed, large-scale, one-to-three stage rig, designed after modern compressors, see Fig. 1 and Hsu and Wo (1998). Flow enters the compressor through a bell-mouth contraction and into the constant blade height annulus. The IGV trailing edge is located 1.75 chord upstream of the rotor leading edge to allow for wake dissipation. The blades were designed using controlled diffusion concept of Hobbs and Weingold (1984). Two special features are designed in the rig: axial gaps between blade rows are variable, from 10% to 60% chord, and the clocking position between rotor rows can be adjusted. In this work, the rotor/stator compressor configuration was tested, as sketched in Fig. 2. (The dash lines defined the blade relative position at time t/T= 0.0 in an unsteady period.) Figure 3 shows the measured static-to-static pressure rise characteristic for rotor/stator and rotor/stator/rotor configurations with varying axial gaps.

四、結果與討論

4.1 Rotor/Stator Compressor Basic Flow

Before we discuss the rotating stall characteristic, it is wise to discuss the pre-stall flow features of this compressor. The rotor/stator configuration includes the effect of (a) rotor wake impinging upon the stator and subsequent wake convection along the stator passage and (b) the potential field of the rotor on the stator. Results due to these two phenomena follow for two axial gaps, Gap1= 10% and 30% chord.

Figure 4 presents the transverse vortical and potential gusts decomposed from slanted hot-wire data using the procedure described in Hsu and Wo (1998) (also see Chung and Wo (1997), which used Navier-Stokes results where Hsu and Wo used experimental data). The hot-wire was located axially upstream of the stator leading edge at the mid-gap position for both 10% and 30% chord gap cases.

The vortical gust signature shows an abrupt increase as the wake passes, which is the dominant feature for both gap cases. The vortical contribution essentially represents the total (prior to decomposition) transverse gust, since the potential contribution is small even at 10% chord gap between blade rows. Figure 4 thus provides further justification for using wake/blade calculation to model the unsteady effect from the upstream blade on the downstream blade (e.g., Giles, 1988 and Hall and Crawley, 1989). Moreover, the distinct difference in time scale between the vortical and potential gusts – the vortical gust on the order of passing of the wake width and the potential gust being blade-to-blade period – can be clearly seen.

It is important to note the time when the gust reaches a maximum since phase information is vital. Location ‘a’ represents the maximum value of the potential gust which occurs at t/T= 1.0, or 0.0 – this coincides with the time instant when the rotor trailing edge is axially forward of the stator leading edge. The location marked ‘b’ represents the instant when the vortical gust is largest, which occurs at the time when the wake passes the hot-wire. Thus, the maximum vortical gust occurs when the rotor wake passes and the maximum potential gust occurs when the rotor blade itself passes. The reason that the time occurrence of location ‘a’ precedes that of ‘b’ is due to the rotor exit flow angle.

4.2 Unstable Flow Characteristics

As stated earlier, the purpose of the study was to make initial attempt to characterize the overall phenomenon of rotating stall by measurement of hot-wire signature upstream of the rotor row. Due to the nature of the rotating stall measurement using the slanted hot-wire was not feasible. Thus measurement was resorted to standard hot-wire technique (using straight hot-wire).

Measurement was taken at reduced flow coefficient of approximately 0.53 with rotor/stator blade configuration, as before. Care was taken by slowing reducing the throttle so that the flow enters into rotating stall naturally. Data acquisition was

commenced as soon as the desired throttle setting was reached, which is slightly below the known stall flow coefficient of 0.53. This was to ensure that the precursor was properly captured. For safety reason (rotating stall can cause large unsteady stresses on blades), the compressor was tested at reduced speed of 525 RPM, which is justified on the ground that since rotating stall occurs at all speeds. The hot-wire was placed at one chord upstream of the rotor leading edge plane.

Data of Fig. 5 show clear characteristic of time-mean steady flow entering into rotating stall flow. The precursor region shows a clear growth of the instability and finally developing into a full-scale rotating stall phenomenon. The frequency of the stall cell is shown to be 0.93 that of the shaft frequency, which means that one stall cell per rev characterize this axial compressor. Moreover the signature of the hot-wire suggests that the spatial extent of the stall cell is fairly small, since there exist a sharp velocity 'dip' during each instant when the hot-wire passes the stall cell. Overall, this is believed to be a reasonable rotating stall characteristic of an axial compressor like one tested.

五、結論

This work sets out to measure the rotating stall flow feature of an axial compressor. The hot-wire was located at one chord upstream of a rotor/stator axial compressor. Measurement was taken at reduced flow coefficient with rotor/stator blade configuration. Data show clear characteristic of time-mean steady flow entering into rotating stall flow. The precursor region shows a clear growth of the instability and finally developing into a full-scale rotating stall phenomenon. The frequency of the stall cell is shown to be 0.93 that of the shaft frequency, which means that one stall cell per rev characterize this axial compressor.

六、參考文獻

Chung, M.H. and Wo, A.M., 1997, "Navier-Stokes and Potential Calculations of Axial Spacing Effect on Vortical and Potential Disturbances and Gust Response in an Axial Compressor," ASME J. Turbomachinery, Vol. 119, No. 3, pp. 472-481.

Doebelin, E.O., 1990, Measurement Systems: Application and Design, 4th ed., McGraw-Hill, p. 482.

Giles, M.B., 1988, "Calculation of unsteady wake/rotor interaction," *J. of Propulsion and Power*, Vol. 4, pp. 356 - 362.

Greitzer, E. M. 1976, "Surge and Rotating Stall in Axial Flow Compressors Part 1: Theoretical; Compression System Model; Part II: Experimental Results and Comparison With Theory," ASME Journal of Engineering for Power, Vol. 98, pp. 190-216.

Hall, K. and Crawley, E., 1989, "Calculation of unsteady flows in turbomachinery using the linearized Euler equations," *AIAA J.,* Vol. 27, No. 6, pp. 777 - 787.

Hobbs, D.E. and Weingold, H.D., 1984, "Development of controlled diffusion aerofoils for multistage compressor applications," J. Eng. for Gas Turbine & Power, Vol. 106, pp. 271-278.

Hsu, S.T. and Wo, A.M., 1988, "Reduction of Unsteady Blade Loading by Beneficial Use of Vortical and Potential Disturbances in an Axial Compressor with Rotor Clocking," ASME J. of Turbomachinery, Vol. 120, No. 4, pp. 705-713.

Lavrich, P. L., 1988, "Time Resolved Measurements of Rotating Stall in Axial Flow Compressors," Ph.D. Thesis, Dept. of Aeronautics and Astronautics, M.I.T., Cambridge, MA.

Schmidt, D. P., and Okiishi, T. H., 1977," Multistage Axial-Flow Turbomachine Wake Production, Transport, and Interation," AIAA Journal, Vol.15, pp.1138-1145.

Wo, A.M. and Bons, J., 1994, "Flow Physics Leading to System Instability in a centrifugal Pump," ASME *Journal of Turbomachinery*, Vol. 116, No. 4, pp. 612-620.

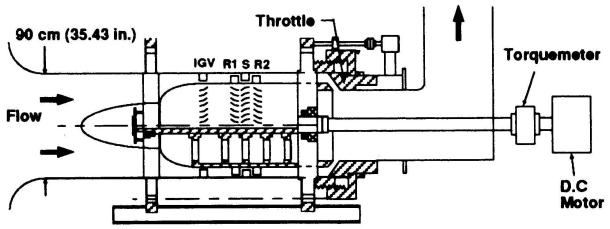

Fig. 1 The Axial Compressor Research Facility used to test the rotor/stator configuration.

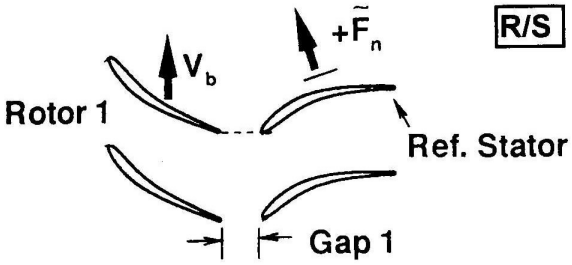

Fig. 2 Rotor/stator configuration at time t/T= 0.0; rotor trailing edge is axially upstream of the stator leading edge. Direction of *positive* stator force, normal to chord, is also shown.

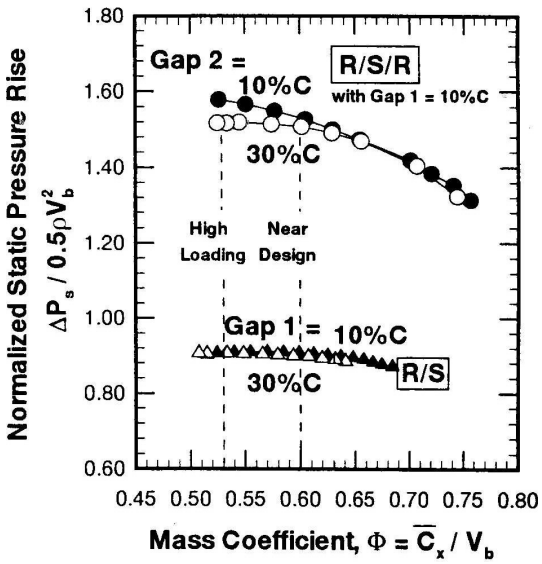

Fig. 3 Measured static-to-static pressure rise characteristic for rotor/stator and rotor/stator/rotor configurations with varying axial gaps.

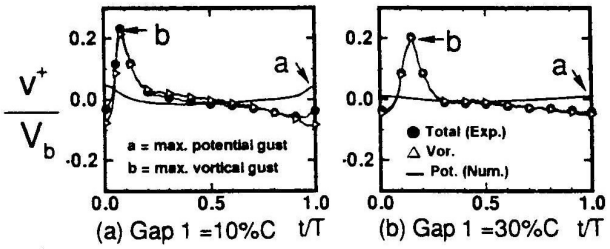

Fig. 4 Vortical and potential transverse gusts at the mid-gap point axially upstream of the stator leading edge (R/S).

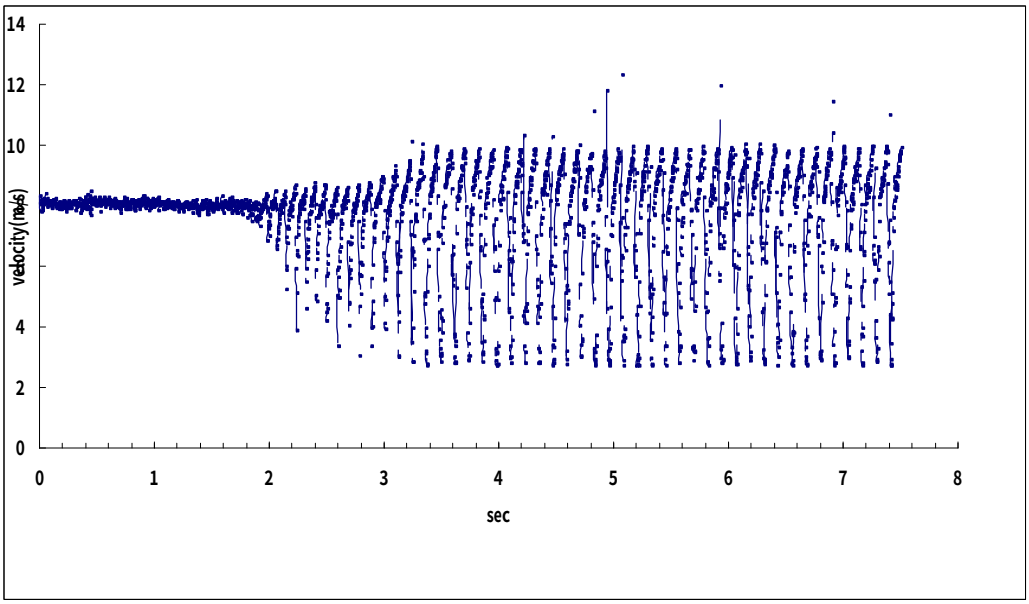

Fig. 5 Rotating stall phenomenon in an axial compressor. The hot-wire was located at one chord upstream of the rotor of a rotor/stator compressor.